Qualitative and Quantitative Anatomy of the Humeral Attachment of the Pectoralis Major Muscle and Structures at Risk

A Cadaveric Study

Phob Ganokroj,*† MD, Kaare Midtgaard,*‡ MD, Bryant P. Elrick,*§ MD, Rony-Orijit Dey Hazra,* MD, Brenton W. Douglass,* MD, Philip C. Nolte,* MD, Annalise M. Peebles,* BA, Brad W. Fossum,* BA, Justin R. Brown,* MD, Peter J. Millett,‖ MD, MSc, and CAPT Matthew T. Provencher,*‖¶ MD, MBA, CAPT, MC, USNR(Ret)

Investigation performed at Steadman Philippon Research Institute, Vail, Colorado, USA

Background: Surgical pectoralis major (PM) repair can offer improved functional outcomes over nonoperative treatment. However, there is a lack of literature on consensus of the anatomical site of the humeral attachment.

Purpose: To provide qualitative and quantitative anatomic analysis of the PM by focusing on humeral insertion and relevant structures at risk.

Study Design: Descriptive laboratory study.

Methods: Eight fresh-frozen male cadavers were dissected. The relevant landmarks that were collected and measured included (1) PM footprint length at the humeral insertion (total, sternal head, and clavicular head insertions); (2) PM tendon length from the humeral insertion to the musculotendinous junction; (3) distance from the PM humeral insertion to the lateral (LPN) and medial (MPN) pectoral nerves; and (4) distance from the coracoid process to the musculocutaneous nerve (MCN) in anatomical position.

Results: The total PM footprint length was 81.4 mm (95% CI, 71.4-91.3). The sternal and clavicular heads that make up the PM had footprint lengths of 42.1 mm (95% CI, 32.9-51.4) and 56.6 mm (95% CI, 46.5-66.7), respectively. The PM tendon was wider at the clavicular head (74.7 mm; 95% CI, 67.5-81.7) than the sternal head insertions (43.0 mm; 95% CI, 40.1-45.9). The distances from the PM humeral insertion to LPN and MPN were 93.2 mm (95% CI, 83.1-103.3) and 103.8 mm (95% CI, 98.3-109.4), respectively. The coracoid process to MCN distance was 68.5 mm (95% CI, 60.2-76.8).

Conclusion: This study successfully quantifies anatomic dimensions of the PM tendon, its sternal and clavicular head insertions, and its location relative to nearby vital structures. Such knowledge can provide surgeons with a better understanding of the PM in relation to nearby neurovascular structures during anatomic PM repair and reconstruction to avoid debilitating complications.

Clinical Relevance: Knowledge of the quantitative anatomy of the PM at the humeral footprint along structures at risk may aid surgeons with identifying the injured part of the PM and improve outcomes for anatomic repair and reconstruction.

Keywords: shoulder anatomy; pectoralis major tendon; humeral insertion and anatomic footprint

Pectoralis major (PM) tendon tears have increased in prevalence because of the growing popularity of sport-related activities and weight training. Young men with an active lifestyle have a higher risk of PM tear with an incidence of 60 per 100,000 person-years.[2,12] Although PM injuries are frequently reported in younger, active populations, the incidence in the elderly population is likely underreported.[3,12]

A bimodal age distribution exists for diagnosis of PM injury, with indirect trauma being the major mechanism for injury.[3,12] This occurs when the shoulder is abducted and externally rotated during activities such as performing bench-press exercises.[1,12,24] The most common type of PM injury is complete rupture at the humeral attachment, followed by ruptures at the musculotendinous junction and ruptures within the muscle belly.[1,12] Repair of PM tendon ruptures can improve functional outcomes compared with nonoperative treatment, especially in athletes and those who undergo surgical repair within 6 weeks of injury.[9,10,25]

The Orthopaedic Journal of Sports Medicine, 10(9), 23259671221121333
DOI: 10.1177/23259671221121333

The PM tendon and muscle may also be used in reconstructive surgery as a complete or split-thickness tendon transfer.[14]

PM muscle resides on the anterior chest wall and facilitates adduction, internal rotation, and flexion of the humerus. The PM is divided into 2 parts: a clavicular head (CH) and the sternal head (SH). There are extensive differing opinions regarding the number of PM muscle segments and tendon layers. There is also little consensus on the folding or twisting of the PM muscle fibers leading to the insertion at the humerus, the humeral footprint of the PM tendon, and the related neurovascular structures from previous studies.[4,7,8,12,13,15,16,18] There is also a lack of agreement on the humeral footprint and therefore where anatomic PM repair should occur.[5,25] Acknowledging and characterizing the complex anatomy of the PM is important at the humeral attachments and nearby neurovascular structures for improving anatomical PM repair (partial and complete repair) and reconstruction.

The study aims were to provide a qualitative and quantitative anatomic analysis of the PM by focusing on the humeral footprint and relevant neurovascular structures at risk during surgical repair or when the tendon is harvested as part of a tendon transfer procedure.

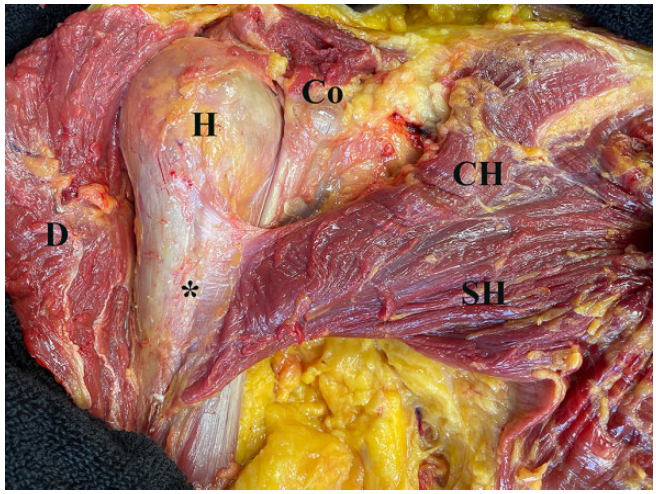

Figure 1. Anatomy of the pectoralis major (PM) (right shoulder) after removing skin, subcutaneous tissue, and deltoid (D). There were 2 heads of the PM muscle (CH and SH) that inserted into the humerus (H) (*) in a bilaminar fashion. These 2 heads of the PM tendon were flat and fused at the level of the musculotendinous junction. CH, clavicular head of the PM; Co, coracoid process; SH, sternal head of the PM.

METHODS

Specimen Preparation

Eight nonpaired, fresh-frozen male cadaveric chests (mean age, 57.9 years; range, 51-66 years) were utilized in this anatomic study. The exclusion criteria comprised no prior chest injury, no metastasis to bone, no gross deformities, and no history of surgery. The specimens were donated for medical research and subsequently purchased by our institution from corresponding tissue banks. Cadaveric studies do not require institutional review board approval at our facility. Before preparation, all specimens were stored at –20°C and thawed at room temperature for 24 hours. All skin and subcutaneous tissue was removed. Superficial muscle was meticulously dissected to expose and clearly identify the entirety of the PM (SH and CH) and its proximal and distal portions and corresponding tendon insertion points on the proximal humerus (Figure 1). After reflecting the tendonous insertion of the PM, the medial pectoral nerve (MPN) and lateral pectoral nerve (LPN) were traced to where they pierced the PM muscle. The conjoint tendon and musculocutaneous nerve (MCN) were identified and sectioned out (Figure 2). During the course of dissection, specimens were kept hydrated with normal saline.

Data Collection

The SH and CH of the PM tendon were identified and sharply dissected down to the bony insertion on the humerus (Figure 1). In order to measure the footprint of the PM tendonous insertion on the humerus, the remaining soft tissue was removed, and the bony landmarks were

¶Address correspondence to CAPT Matthew T. Provencher, MD, MBA, CAPT, MC, USNR(Ret), Steadman Philippon Research Institute and The Steadman Clinic, 181 West Meadow Drive, Suite 400, Vail, CO 81657, USA (email: mprovencher@thesteadmanclinic.com) (Twitter: @drprovencher, @SteadmanClinic).

*Steadman Philippon Research Institute, Vail, Colorado, USA.

†Faculty of Medicine Siriraj Hospital, Mahidol University, Bangkok, Thailand.

‡Division of Orthopaedic Surgery, Oslo University Hospital, Oslo, Norway.

§Department of Orthopedics, University of Colorado School of Medicine, Aurora, Colorado, USA.

‖The Steadman Clinic, Vail, Colorado, USA.

Final revision submitted May 13, 2022; accepted July 5, 2022.

One or more of the authors has declared the following potential conflict of interest or source of funding: Specimens were donated for medical research and subsequently purchased by the Steadman Philippon Research Institute (SPRI) from corresponding tissue banks. P.J.M. has received research support from Arthrex, Ossur, Siemens, and Smith & Nephew; consulting fees from Arthrex; royalties from Arthrex, Medbridge, and Springer; hospitality payments from Arthrosurface, Merz Pharmaceuticals, Sanofi-Aventis, and Stryker; and stock/stock options from VuMedi. M.T.P. has received consulting fees from Arthrex, JRF Ortho, and SLACK; royalties from Arthrex and Elsevier; and honoraria from Arthrosurface. The SPRI, a 501(c)(3) nonprofit institution supported financially by private donations and corporate support, exercises special care to identify any financial interests or relationships related to research conducted. During the past calendar year, SPRI has received grant funding or in-kind donations from Arthrex, Ossur, Siemens, Smith & Nephew, and DJO. AOSSM checks author disclosures against the Open Payments Database (OPD). AOSSM has not conducted an independent investigation on the OPD and disclaims any liability or responsibility relating thereto.

Ethical approval was not sought for the present study.

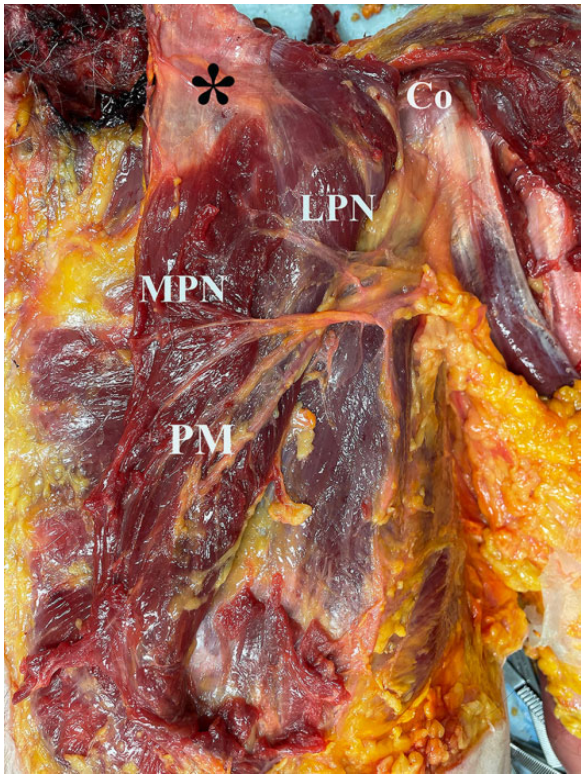

Figure 2. Anatomy of the related neurovascular structures (left shoulder) after cutting the humeral insertion of the pectoralis major (PM) (*). The distance between points was measured with calipers starting from the humeral insertion of the PM tendon (*) to the closest nerve bundles (MPN and LPN) that entered the PM muscle. Co, coracoid process; LPN, lateral pectoral nerve; MPN, medial pectoral nerve.

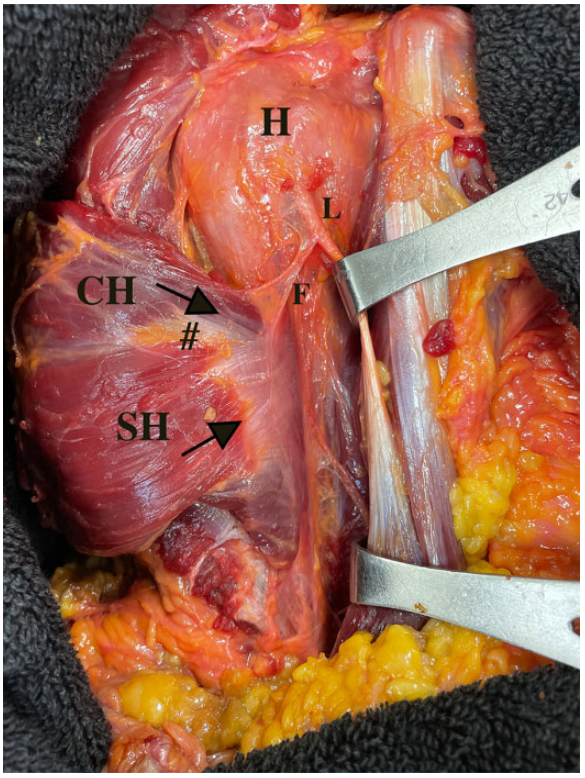

Figure 3. The posterior surface of the pectoralis major (PM) humeral insertion after reflecting the muscle (right shoulder). After reflecting the PM muscle to the posterior surface, these 2 head insertions could be distinguished by an interposed fat pad (#) and display the 2 directions (arrows) of tendon insertion layers. The falciform ligament or the fibrous expansion of the PM tendon was identified in all specimens. This ligament could be clearly distinguished from the SH of the PM. CH, clavicular head of the PM; F; falciform ligament; H, humerus; L, long head of biceps tendon; SH, sternal head of the PM.

exposed. A joint coordinate frame was established using a coordinate measuring machine (Romer Absolute Arm; Hexagon Manufacturing Intelligence) in accordance with the methodology established by SimVITRO. The robotic arm used in this study has ±0.025 mm of point repeatability and ±0.037 mm of volumetric accuracy, and variability among specimens was minimal.[22] Collected landmarks on the humerus included the proximal and distal points of the SH and CH insertions of the PM, which were used to calculate the total PM footprint length (superior to inferior) as well as SH and CH insertions of PM footprint lengths (Figures 3 and 4). Next, these 2 heads of the PM tendon were identified and measured the tendon length (from the humeral insertion to the musculoskeletal junction) with a caliper.

After cutting the humeral insertion of the PM tendon, the distances starting from the center of the humeral insertion of the PM tendon to the closest nerve bundles (MPN and LPN) that entered the PM muscle were measured with calipers (Figure 2). Then, the origin of the conjoint tendon comprising the short head of biceps and coracobrachialis was measured to the point where MCN enters the coracobrachialis muscle. All cadavers were measured in the supine position with the arm at the side of the body (0° of flexion and abduction with neutral rotation) and the palm facing forward. All measurements were performed by 2 examiners at the same time and blinded to each other to determine the interclass correlation coefficient (ICC) for internal consistency (P.G. and K.M.).

Data Analysis

The coordinates of the collected points were imported into MATLAB (Version R2021a, The MathWorks Inc., Natick, MA) script for analysis. The distance between landmarks was calculated as a direct linear distance between 2 collected points to determine the PM tendon footprint length (SH, CH, and total PM tendon insertion lengths) (Figure 4). The distance between the proximal point of 2 head insertions and the overlapping distance were also calculated (Figure 4). Descriptive statistical analysis was performed to include means with 95% CIs. Distances were reported in millimeters. The interrater reliability of the measurement was assessed via the ICC using the bootstrapping method. Based on the 95% CI of the ICC, the reliability values were

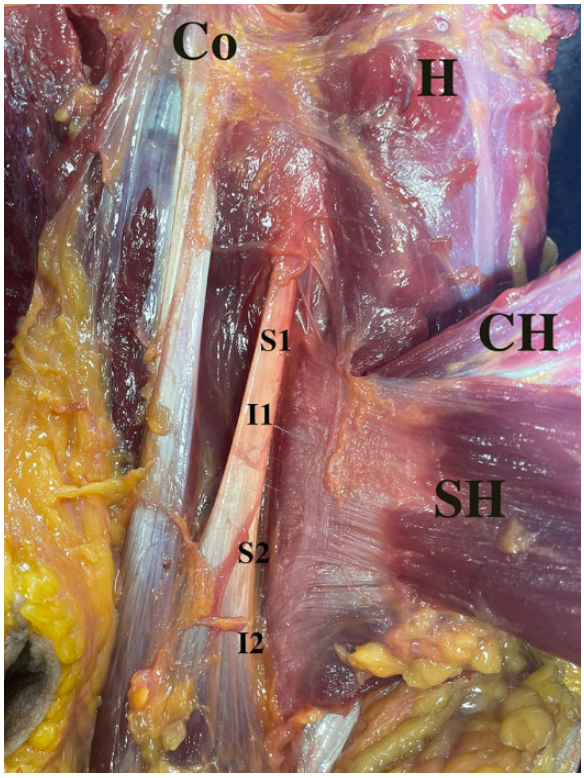

Figure 4. The posterior surface of the pectoralis major (PM) humeral insertion after reflecting the muscle (left shoulder). Landmarks on the humerus included the proximal and distal points of the SH (S1, S2) and CH insertions (I1, I2). The total PM footprint length is calculated from S1 to I2, and the SH and CH of PM tendon footprint lengths (S1 to S2 and I1 to I2, respectively). The distance from the proximal border of the SH insertion to the proximal border of the CH insertion of the PM (S1 to I1), and the overlapping distance between these 2 head insertions (I1 to S2). H, humerus; CH, clavicular head of the PM; Co, coracoid process; I1 and I2, the proximal and distal points of clavicular head insertion; S1 and S2, the proximal and distal points of sternal head insertion; SH, sternal head of the PM.

classified as excellent (ICC, ≥0.9), good (ICC, 0.75-0.89), fair (ICC, 0.5-0.74), or poor (ICC, <0.5).[20] Statistical analyses were performed using the statistical software SPSS for Windows (Version 18.0; SPSS Inc) and R Version 4.1.2 (R Foundation for Statistical Computing).

RESULTS

Qualitative Anatomy

There were 2 heads of the PM muscle (CH and SH) that inserted into the humerus in a bilaminar fashion. The SH of the PM muscle coursed from inferomedial to superolateral and inserted at the lateral lip of the intertubercular sulcus of the humerus (Figure 1). The CH of the PM muscle coursed in a superomedial-to-inferolateral direction (Figure 1). These 2 head insertions of the PM tendon were flat and fused at the level of the musculotendinous junction. The fused head insertions could not be separated from the anterior aspect of the humerus by a blunt dissection. However, after reflection of the PM muscle to expose the posterior surface, these 2 head insertions of the PM tendon could be determined by an interposed fat pad and a disparity between 2 directions of tendon insertion layers as mentioned above (Figure 3). In all specimens, there was no clear evidence of folding or twisting of either the SH or CH of the PM tendon under direct visualization.

During dissection, the falciform ligament or the fibrous expansion of the PM tendon was identified in all specimens. It formed an oblique fiber orientation from the SH insertion of the PM to the lateral aspect of the bicipital groove. This ligament could be clearly distinguished from the SH of the PM and should be excised to clearly identify the PM footprint on the humerus (Figure 3).

TABLE 1
Distance Measurements Between PM Insertion Points on the Humerus[a]

Measurement PM Footprint Length (Superior to Inferior)	Distance, mm
SH insertion of PM tendon	42.1 (32.9-51.4)
CH insertion of PM tendon	56.6 (46.5-66.7)
Distance from proximal border of SH-to-CH insertions of PM tendon	24.9 (11.92-38.0)
Overlapping tendon (between SH and CH insertions)	27.9 (18.4-37.5)
Total PM insertion	81.4 (71.4-91.3)

[a]Data are presented as mean (95% CI). CH, clavicular head of the PM; PM, pectoralis major; SH, sternal head of the PM.

Quantitative Anatomy

The total footprint length of the PM tendon (from superior to inferior) on the humeral insertion was 81.4 mm (95% CI, 71.4-91.3). The footprint length of the SH was shorter than the CH insertions of the PM, 42.1 mm (95% CI, 32.9-51.4) and 56.6 mm (95% CI, 46.5-66.7), respectively (Table 1). The distance from the proximal border of the SH to CH insertions of the PM was 24.9 mm (95% CI, 11.9-38.0), with an overlap between these 2 insertion layers of 27.9 mm (95% CI, 18.4-37.5) (Table 1).

The tendon length (from the humeral insertion to the musculotendinous junction) of the SH insertion of the PM was narrower than the CH insertion of the PM, 43.0 mm (95% CI, 40.1-45.9) and 74.7 mm (95% CI, 67.5-81.7), respectively (Table 2). The closest distances from the humeral insertion to the adjacent neurovascular structures are listed in Table 2. From the PM humeral insertion, the LPN and MPN pierced the PM muscle at means of 93.2 mm (95% CI, 83.1-103.3) and 103.8 mm (95% CI, 98.3-109.4), respectively (Table 2). The ICC values were excellent at 0.963 (95% CI, 0.804-0.982) for interobserver reliability.

TABLE 2
PM Tendon Length and Distance Measurements Between the Humeral Footprint and the Adjacent Neurovascular Structures[a]

Measurement	Distance, mm
SH insertion tendon length	43.0 (40.1-45.9)
CH insertion tendon length	74.7 (67.5-81.7)
PM humeral insertion to LPN	93.2 (83.1-103.3)
PM humeral insertion to MPN	103.8 (98.3-109.4)
Coracoid process to MCN	68.5 (60.2-76.8)

[a]Data are presented as mean (95% CI). The PM tendon length was measured from the humeral insertion to the musculotendinous junction. CH, clavicular head of the PM; LPN, lateral pectoral nerve; MCN, musculocutaneous nerve; MPN, medial pectoral nerve; PM, pectoralis major; SH, sternal head of the PM.

DISCUSSION

The principal findings of this study demonstrated that the entirety of the PM footprint length was 81.4 mm (95% CI, 71.4-91.3). Such findings will improve quantitative familiarity for relevant structures that can be applied during anatomical repair or PM reconstruction in a chronic or irreparable PM tear (partial or complete). The reported PM footprint length in the current study is notably greater than that in previous studies, in which the weighted-mean PM tendon length was 62.5 mm.[4] In previous literature, there was a large range of PM footprint length spanning from 24 to 97 mm. Variables that may contribute to the wide range of these values include the method of measurement, types of cadaver, and points of measurement. The authors also chose all male cadavers in this study, which may be associated with a higher PM footprint length than other studies. In terms of clinical relevance, the findings from the current study highlight that adequate exposure is essential to facilitate an anatomic repair or reconstruction of the broad footprint length of the PM. This has clinical implications and has been used by some authors in split-thickness PM tendon transfers where the SH principally is transferred for a deficient subscapularis.[14] It also has clinical implications in acute PM tendon tears, as the SH tears more commonly and can easily be missed if the surgeon only sees the intact CH layer.

There were 2 heads of the PM tendon that were identified in this study. These 2 head insertions were flat and fused at the level of musculotendinous junction. The CH insertion was longer than the SH insertion, with measurements of 56.6 and 42.1 mm, respectively. The footprint length of tendon overlap was measured at 27.9 mm. In a previous study, Jennings et al[17] found 2 laminae of the PM at the humeral footprint, which were described as the anterior and posterior laminae. The anterior lamina consisted of the tendon from the clavicular portion of the PM. The anterior lamina was found to be longer than the posterior lamina (sternal portion of the PM), which was measured to be 43.0 mm. The measurement for the overlap of these 2 laminae was 27 mm (range, 1-56 mm).[17]

Jennings et al[17] found an isolated CH of the PM but could not differentiate between each segment of the SH in their study. In previous studies, 1 to 3 layers of PM tendons were found at the humeral footprint.[11,13,16,17,26] Huang et al[16] completed a PM tendon anatomical study using magnetic resonance imaging (MRI), ultrasound, and histologic investigation. Their team illustrated that the 2 heads of the PM muscle were CH and SH but had a unilaminar presentation on both gross inspection and histologic enthesis.[16] We also found that the SH and CH insertions of the PM merged into a single tendon at the humeral insertion in this study. These insertional heads can be differentiated by the interposed fat pad and the tendon's direction at the posterior surface of the humeral insertion of the PM. Such findings are similar to the 3-dimensional study of the PM muscle and tendon architecture by Fung et al,[13] who found that the 2 layers at the humeral PM tendon fused before its insertion at the humeral footprint. From their study, the posterior layer was composed of lower segments of SH and inserted on the humerus superior to the anterior layer.[13] The findings from the current study support the bilaminar concept of the PM tendon at the humeral insertion.

Previous studies have found that the population with the highest prevalence of chronic PM tendon injuries was male.[20] Kowalczuk et al[21] found that these chronic tears most commonly occurred between the musculotendinous junction and the humeral tendinous insertion. Partial-thickness and complete-width tears were the most common type of tear pattern.[12,21] MRI is the investigation of choice for characterization of tear pattern and preoperative evaluation.[5] A combination of the bilaminar characteristics and overlapping of the PM tendon insertion on the humerus makes it difficult to characterize the partial tear using MRI.[6,7] The current study also found that it was difficult to differentiate between SH and CH during direct inspection of the humeral insertion at the anterior surface. The authors propose that using the distance from the proximal border of the SH insertion may be useful for determining which portion of the PM was injured. In this study, the proximal part of the CH insertion was 25 mm (1 inch) below the proximal part of the SH insertion. Injury or tear below this point might represent a complete tear of the PM tendon and will guide surgeons to perform an anatomic repair or reconstruction for both portions of the PM tendon (CH and SH). When increasing surgical exposure in a proximal humeral surgery, surgeons should be aware not to release the proximal part of the PM more than 25 mm, as doing so may cause injury to both the CH and the SH of the PM humeral insertion.

The current study found that the length (medial to lateral) of the CH insertion was wider than the SH insertion, with measurements being 74.7 mm and 43.0 mm, respectively. Previous literature found that either the posterior lamina (SH) tendon length was wider than the anterior lamina (CH) or there was no difference in tendon length between the 2 laminae.[13,17] Variability in these results can be explained by multiple factors. These include the method of measurement (3-dimensional digital model or caliper), types of cadavers (formalin embalmed or fresh-frozen), and points of measurement. The authors of the present study

found 2 distinct head insertions (SH and CH) with different lengths and orientations. For total-length PM tears or chronic tears requiring allograft augmentation, a longer graft or 2 distinct graft reconstructions may be possible options for achieving anatomical PM reconstruction.

The distances measured in the current study from the PM tendon humeral insertion to LPN and MPN were of similar values when compared with previous studies. The humeral insertion to LPN was 93.2 mm in the current study compared with 125 mm in previous studies, and the humeral insertion to MPN measured 103.8 mm compared with 93 to 119 mm in the literature.[17,19] There is little to no reporting of cases in the current literature for LPN or MPN injury during PM repair or reconstruction. The safe zone measured in this study was >90 mm from the humeral insertion. For chronic cases, care should be taken to avoid vigorous dissection when mobilizing retracted tendon.[5,23] For the MCN, this study found that the distance from the coracoid process to the first branch of MCN piercing the coracobrachialis was 68.5 mm. In a similar study, Klepps et al[19] found that the safe distance from the coracoid process to the proximal branch of MCN was 44 mm (range, 14-74 mm). Klepps et al showed that transferring PM superficial to the MCN created less nerve tension when compared with transferring PM deep to the MCN. This team recommended MCN exploration during operation because of the high variability and location of MCN, in order to prevent tension on the nerve. PM repair or reconstruction around this footprint area remains a safe zone for surgery; however, thorough knowledge of the anatomy in this area will help surgeons avoid complications.

Limitations

This study had several limitations that are commonly observed in cadaveric studies. The limited number of cadavers, monoethnicity, and all specimens being male may influence the generalizability of the results. The nonpaired, fresh-frozen male cadavers analyzed in this study translated to the population with a higher incidence of PM tendon injury. Applying these findings to a female population should be done with caution. Measurement error is also a primary concern because of the nature of the anatomical study. All measurements in this study were done by 2 examiners, and the calculated ICC values were excellent for internal consistency. This study used the coordinate measuring machine to achieve more accuracy and less variability for the anatomy of the humeral attachment of the PM in order to reduce the measurement error. Future studies should focus on the differences in clinical outcome between repair of partial or complete footprint lengths of the PM tendon, along with single- versus double-bundle PM reconstructions.

CONCLUSION

This study successfully quantifies anatomic dimensions of the PM tendon, its humeral head insertion (SH and CH), and its location relative to nearby vital structures. Such knowledge can provide surgeons with a better understanding of the PM in relation to nearby neurovascular structures during anatomic PM repair and reconstruction to avoid debilitating complications.

ACKNOWLEDGMENT

The authors gratefully thank Ms. Narumol Sudjai for the statistical analysis and Ms. Waraporn Chalermsuk for graphic materials.

REFERENCES

1. Bak K, Cameron EA, Henderson IJ. Rupture of the pectoralis major: a meta-analysis of 112 cases. *Knee Surg Sports Traumatol Arthrosc*. 2000;8(2):113-119.
2. Balazs GC, Brelin AM, Donohue MA, et al. Incidence rate and results of the surgical treatment of pectoralis major tendon ruptures in active-duty military personnel. *Am J Sports Med*. 2016;44(7):1837-1843.
3. Beloosesky Y, Grinblat J, Weiss A, et al. Pectoralis major rupture in elderly patients: a clinical study of 13 patients. *Clin Orthop Relat Res*. 2003;413:164-169.
4. Bois AJ, Lo IKY. Surgical anatomy of the pectoralis major tendon insertion revisited: relationship to nearby structures and the pectoral eminence for defining the anatomic footprint. *JSES Int*. 2020;4(2):324-332.
5. Butt U, Mehta S, Funk L, Monga P. Pectoralis major ruptures: a review of current management. *J Shoulder Elbow Surg*. 2015;24(4):655-662.
6. Chang ES, Zou J, Costello JM, Lin A. Accuracy of magnetic resonance imaging in predicting the intraoperative tear characteristics of pectoralis major ruptures. *J Shoulder Elbow Surg*. 2016;25(3):463-468.
7. Chiavaras MM, Jacobson JA, Smith J, Dahm DL. Pectoralis major tears: anatomy, classification, and diagnosis with ultrasound and MR imaging. *Skeletal Radiol*. 2015;44(2):157-164.
8. David S, Balaguer T, Baque P, et al. The anatomy of the pectoral nerves and its significance in breast augmentation, axillary dissection and pectoral muscle flaps. *J Plast Reconstr Aesthet Surg*. 2012;65(9):1193-1198.
9. de Castro Pochini A, Andreoli CV, Belangero PS, et al. Clinical considerations for the surgical treatment of pectoralis major muscle ruptures based on 60 cases: a prospective study and literature review. *Am J Sports Med*. 2014;42(1):95-102.
10. de Castro Pochini A, Ejnisman B, Andreoli CV, et al. Pectoralis major muscle rupture in athletes: a prospective study. *Am J Sports Med*. 2010;38(1):92-98.
11. de Figueiredo EA, Terra BB, Cohen C, et al. The pectoralis major footprint: an anatomical study. *Rev Bras Ortop*. 2013;48(6):519-523.
12. ElMaraghy AW, Devereaux MW. A systematic review and comprehensive classification of pectoralis major tears. *J Shoulder Elbow Surg*. 2012;21(3):412-422.
13. Fung L, Wong B, Ravichandiran K, et al. Three-dimensional study of pectoralis major muscle and tendon architecture. *Clin Anat*. 2009;22(4):500-508.
14. Gerber A, Clavert P, Millett PJ, Holovacs TF, Warner JJP. Split pectoralis major and teres major tendon transfers for reconstruction of irreparable tears of the subscapularis. *Tech Shoulder Elb Surg*. 2004;5(1):5-12.
15. Haładaj R, Wysiadecki G, Clarke E, Polguj M, Topol M. Anatomical variations of the pectoralis major muscle: notes on their impact on pectoral nerve innervation patterns and discussion on their clinical relevance. *Biomed Res Int*. 2019;2019:6212039.
16. Huang BK, Wong JH, Haghighi P, et al. Pectoralis major tendon and enthesis: anatomic, magnetic resonance imaging, ultrasonographic, and histologic investigation. *J Shoulder Elbow Surg*. 2020;29(8):1590-1598.
17. Jennings GJ, Keereweer S, Buijze GA, De Beer J, DuToit D. Transfer of segmentally split pectoralis major for the treatment of irreparable

rupture of the subscapularis tendon. *J Shoulder Elbow Surg*. 2007; 16(6):837-842.
18. Katsuki S, Terayama H, Tanaka R, et al. Variation of insertion of the pectoralis major in a cadaveric study: a case report. *Medicine (Baltimore)*. 2020;99(31):e21475.
19. Klepps SJ, Goldfarb C, Flatow E, Galatz LM, Yamaguchi K. Anatomic evaluation of the subcoracoid pectoralis major transfer in human cadavers. *J Shoulder Elbow Surg*. 2001;10(5):453-459.
20. Koo TK, Li MY. A guideline of selecting and reporting intraclass correlation coefficients for reliability research. *J Chiropr Med*. 2016;15(2): 155-163.
21. Kowalczuk M, Rubinger L, Elmaraghy AW. Pectoralis major ruptures: tear patterns and patient demographic characteristics. *Orthop J Sports Med*. 2020;8(12):2325967120969424.
22. Moatshe G, Marchetti DC, Chahla J, et al. Qualitative and quantitative anatomy of the proximal humerus muscle attachments and the axillary nerve: a cadaveric study. *Arthroscopy*. 2018;34(3): 795-803.
23. Provencher MT, Handfield K, Boniquit NT, et al. Injuries to the pectoralis major muscle: diagnosis and management. *Am J Sports Med*. 2010;38(8):1693-1705.
24. Rijnberg WJ, van Linge B. Rupture of the pectoralis major muscle in body-builders. *Arch Orthop Trauma Sur*. 1993;112(2):104-105.
25. Thompson K, Kwon Y, Flatow E, et al. Everything pectoralis major: from repair to transfer. *Phys Sportsmed*. 2020;48(1):33-45.
26. Wolfe SW, Wickiewicz TL, Cavanaugh JT. Ruptures of the pectoralis major muscle: an anatomic and clinical analysis. *Am J Sports Med*. 1992;20(5):587-593.